
Neural interval-censored survival regression with feature selection

Carlos García Meixide^{*1,2}, Marcos Matabuena^{**3}, Louis Abraham⁴, and Michael R. Kosorok⁵

¹ Instituto de Ciencias Matemáticas, CSIC

² Departamento de Matemáticas, Universidad Autónoma de Madrid

³ Harvard University

⁴ Université Paris 1 Panthéon-Sorbonne

⁵ University of North Carolina, Chapel Hill

Abstract: Survival analysis is a fundamental area of focus in biomedical research, particularly in the context of personalized medicine. This prominence is due to the increasing prevalence of large and high-dimensional datasets, such as omics and medical image data. However, the literature on non-linear regression algorithms and variable selection techniques for interval-censoring is either limited or non-existent, particularly in the context of neural networks. Our objective is to introduce a novel predictive framework tailored for interval-censored regression tasks, rooted in Accelerated Failure Time (AFT) models. Our strategy comprises two key components: i) a variable selection phase leveraging recent advances on sparse neural network architectures, ii) a regression model targeting prediction of the interval-censored response. To assess the performance of our novel algorithm, we conducted a comprehensive evaluation through both numerical experiments and real-world applications that encompass scenarios related to diabetes and physical activity. Our results outperform traditional AFT algorithms, particularly in scenarios featuring non-linear relationships.

Key words: Survival Analysis; Interval-Censoring; High-dimensional Data; Non-linear Regression; Diabetes research

1 Introduction

In recent decades, interval-censored data modeling has been a subject of intense research from methodological, theoretical, and applied perspectives (van de Geer, 1993; Huang, 1996; Wu and Cook, 2020; Cho et al., 2021). Interval-censoring arises from data collection mechanisms that prevent the target event of a system from being observed directly because it is only known to lie within an observed interval. The boundary elements of these intervals belong to a sequence of examination times or check-ups. This type of data is commonly encountered in various fields including medicine, engineering, and social sciences; requiring specialized statistical methods.

Recently, the first machine learning contributions appeared in the literature, such as specific smoothing random forest algorithms (Cho et al., 2021), a more classical tree ensemble random forest (Yao et al., 2019), gradient boosting (Hothorn et al., 2005), or the first methodology tackling interval-censoring based on kernel machines (Travis-Lumer and Goldberg, 2021). Notably, deep learning algorithms are scarce in this setting (Sun and Ding, 2023) and inexistent in the high-dimensional case, despite the recent progress survival analysis has undergone during the last years with right-censored outcomes (Zhong et al., 2021; Lee et al., 2018; Steingrimsson and Morrison, 2020; Rindt et al., 2022; Jia and Jeong, 2022).

*Corresponding author: e-mail: carlos.garcia@icmat.es

**Corresponding author: e-mail: mmatabuena@hsph.harvard.edu

Although deep learning models hold potential advantages to handle high-dimensional data and non-linear dependencies, extending neural network models to an interval-censoring context- or, more generally, to survival analysis- brings several methodological hurdles. Traditionally, models for regression of interval-censored outcomes are trained by solving complex second-order optimization problems (Zhang et al., 2010). However, first-order methods only train neural networks on strongly non-convex problems (Zhong et al., 2022). Furthermore, many survival analysis models have a semiparametric nature, an area where deep learning literature is scarce in developing both efficient estimators and specific optimization techniques.

The goal of this paper is to propose a modelling framework based on neural networks centered around AFT targeting interval-censored outcomes. The new methodology includes:

1. A sparse neural network architecture for variable selection with interval-censored responses based on (Lemhadri et al., 2021).
2. A flexible predictive algorithm for interval-censored outcomes.

From a technical perspective, AFT can be viewed as the natural generalization of linear regression to the field of survival analysis aiming to model conditional distributions between two random variables $Z \in \mathbb{R}^d$ and $T \in \mathbb{R}$. It has a clear physics motivation and is widely used in practice (Wei, 1992).

Two main lines of research have been developed in the literature. The first involves specifying a parametric law for the noise that characterizes the conditional distribution of the scale and location model (Bagdonavicius and Nikulin, 2001). In the second, the noise distribution is not specified, generally being estimated with nonparametric methods (Pang et al., 2021). However, this approach- popular in the field of right-censoring- poses challenges in potential extensions to the interval-censored case due to identifiability issues and numerical estimation problems. Therefore, during our simulated experiments and case studies, we will assume a parametric noise structure to obtain stable optimization algorithms.

A critical step in our framework, especially in the variable selection case, is to consider (Meinshausen and Bühlmann, 2010)'s stability selection. Stability selection is an alternative strategy for selecting variables in noisy environments, as is the case of our context. Random weight initialization in deep learning computational libraries helps estimating stability paths, contributing to the randomness arising from subsampling. Traditional approaches to selecting structure, such as cross-validation, are difficult to carry out because the initial weights' randomness leads to local minima, which generate discordant solutions for each fold and each structure, making it challenging to assess model stability.

1.1 The difficulty of statistical inference with interval-censored data

The non-parametric estimation of survival functions with interval-censored data is based on (Turnbull, 1976)'s algorithms, derivable with a self-consistency argument (Efron, 1967) which he proved to be also the NPMLE. Significant issues pointed out in the literature are its lack of uniqueness if the log-likelihood is not strictly concave and the fact that consistency results are usually available upon assuming a fixed number of inspection times (Gentleman and Geyer, 1994). (Maathuis and Wellner, 2008) deduce that the NPMLE for the joint distribution function of an interval-censored survival time and a continuous mark variable is not consistent in general. What is more, the self-consistent approach may not be consistent even when the inspection times only take on finitely many values, see counterexample in (Yu et al., 2000). Moreover, traditional methodology in the corpus of computational statistics such as the bootstrap is known to be inconsistent when using the NPMLE as the reference measure with interval-censoring Sen and Xu (2015). Due to these challenges, practitioners often resort to parametric and semi-parametric approaches for modeling interval-censored data that are numerically more stable and yield consistent solutions from both optimization and statistical perspectives. In this paper to introduce more flexibility in the semiparametric modeling, we propose Accelerated Failure Time (AFT) predictive framework using a neural network models.

1.2 Summary of contributions

Our manuscript introduces a novel framework in the field of interval-censored data. The main contributions are discussed below:

1. We present the first variable selection algorithm in interval-censoring based on neural networks, leveraging advances in LassoNet-like architectures (Lemhadri et al., 2021). It is specifically tailored to select the most relevant covariates regarding the conditional survival function of a time-to-event response. Unlike previous approaches in the literature that focused on variable relevance in terms of conditional expectations, our approach concentrates on modeling the conditional survival function in terms of AFT parametric models (Wei, 1992).
2. Variable selection becomes a challenge when estimators depend on numerous hyperparameters and difficult underlying optimization problems may lead to numerical instability, as is the case of neural networks. Similar problems occurred in a less severe way in traditional penalized regression models, as is the case of Lasso (Tibshirani, 1996). Practitioners have used solutions such as stability selection, which possess guarantees on the expected number of false positives under general conditions and from a model-free perspective. Here, we use stability selection (Meinshausen and Bühlmann, 2010) for the first time in the setting of neural networks and empirically validate its applicability and effectiveness.
3. We introduce, from a predictive perspective, a non-sparse architecture that can be stably trained with first-order optimization methods and outperforms traditional AFT models under non-linear ground dependencies.
4. We deduce the analytical expression of a new family of curves that serve to guide practitioners graphically in terms of false discovery rate, see Figure 4.
5. We illustrate the potential of our methodology through relevant biomedical applications. Thanks to the interpretability of AFT models, we obtain new findings in our application studies.
6. The software implementation of our method is freely available for public use and can be accessed through <https://github.com/meixide/spinet>.

1.3 Structure of the paper

The structure of the manuscript is detailed below. In Section 2, we introduce the general form of AFT models for both variable selection and prediction. We also discuss the interval-censored likelihood relevant to our problem and present its optimization scheme. Section 3 presents the results of a simulation study that demonstrates the advantages of our approach followed by a relevant case study related to kidney disorders from the T1D Exchange, a database containing important information on progression of individuals with type 1 diabetes mellitus in the United States. In Section 4, we discuss the methods used, the results obtained, and future research questions raised by our approach. The Supplementary Material contains another relevant application related to the National Health and Nutrition Examination Survey (NHANES), a program of studies designed to assess the health and nutritional status of adults and children in the United States.

2 Methods

Let $T \in [0, +\infty)$ be a random time-to-event response variable and $Z \in \mathbb{R}^d$ a random vector of covariates. We denote by $1 - G(t | z) = P(T > t | Z = z)$ the conditional survival function: the probability of event occurrence before $t \in [0, +\infty)$ given $z \in \mathbb{R}^d$. In this paper, we restrict ourselves to AFT models, which can be expressed as $G(t | z) = F(\phi(t) - r(z))$, where F is a noise distribution to be specified, ϕ is an appropriate monotone function and r is a regression function approximated by elements belonging to a certain space that we will define subsequently.

2.1 “Case-2” interval-censoring

Interval-censoring is an ubiquitous data structure in medical studies, so it has to be faced by predictive models of disease developing. The methodology presented in this paper is specifically tailored for “case 2” interval censoring, which can be used to model more complex schemes. This is because, computationally speaking, the general interval-censoring scheme can be effectively reduced to “case 2” interval-censoring, which makes this approach a practical and powerful tool for handling a wide range of scenarios. We briefly describe three types of interval-censoring mechanisms following (Sun, 2006).

In current status data- also known as “case 1” interval-censoring- the only knowledge about the failure is whether it has occurred or not before an observed checkpoint. “Case k ” interval censoring, $k > 1$, arises when there are k examination times per subject. As a particularization with $k = 2$, in “case 2”, we can only determine that the true failure has occurred either within some random time interval, before the left border of the time interval, or after the right end point of the interval. We insist in that it is not possible to precisely determine the exact time at which the event occurred, but rather we can only observe its possible range of values. Last generalization consists on letting the number of observation instants to vary across individuals. Note that it is convenient to reduce this type of interval-censoring to “case 2” by considering whether the failure occurred before the first examination time, after the last examination time, or between two checkpoints. As we mentioned, this transformation locates “case 2” interval-censoring as a fundamental setting.

Let T_i be the i th patient’s unobservable failure time for $i = 1, \dots, n$. In the framework of interval-censored data T_i will never be observed. In “case 2” interval-censoring scheme, data can be expressed as

$$\left\{ (Z_i, U_i, V_i, \delta_{1i} = 1_{[T_i \leq U_i]}, \delta_{2i} = 1_{[U_i < T_i \leq V_i]}) \right\}_{i=1}^n$$

where $Z_i \in \mathbb{R}^d$ is the vector of observed covariates and $U_i \leq V_i$ a.s. are two independent random checkup time points for individual i . Now, assuming as in Huang and Wellner (1997) that

1. the (unobservable) failure time is independent of the examination times given the covariates
2. the joint distribution of the examination times and the covariates are independent of the parameters of interest

we can write the interval-censored log-likelihood function:

$$\begin{aligned} l_n(\sigma, r) = & \sum_{i=1}^n \left\{ \delta_{1i} \log F \left(\frac{\log U_i - r(Z_i)}{\sigma} \right) \right. \\ & + \delta_{2i} \log \left[F \left(\frac{\log V_i - r(Z_i)}{\sigma} \right) - F \left(\frac{\log U_i - r(Z_i)}{\sigma} \right) \right] \\ & \left. + \delta_{3i} \log \left[1 - F \left(\frac{\log V_i - r(Z_i)}{\sigma} \right) \right] \right\} \end{aligned}$$

where σ is a scale parameter; δ_{1i} , δ_{2i} , and $\delta_{3i} = 1 - \delta_{1i} - \delta_{2i}$ are indicator variables taking the value 1 if the i th observation is left, interval or right censored, respectively. In instances where exact survival times, denoted as T_i , are observed, their contribution to the log-likelihood can be properly expressed as the evaluation of the standard normal probability density function (pdf) at $\frac{\log T_i - r(Z_i)}{\sigma}$.

2.2 Variable selection

2.2.1 Sparse neural networks

Additional architectural constraints are needed to produce sparse estimators in the context of neural networks. In many applications, such as those in medical disciplines, the interpretability of parameter estimates plays a crucial role. Despite their prediction accuracy and generalization ability, deep learning

models are built upon relatively large sets of parameters whose values are not informative for practitioners. With sights on solving this problem, our methodology is inspired by the new neural network sparsity paradigm introduced in (Lemhadri et al., 2021). We depict its architecture in Fig. 2

The regression function involved in the AFT model specified in subsection 2.2 will be approximated by elements $r_{\theta,W} \in \mathcal{R}$, being \mathcal{R} the space of deep residual blocks

$$\mathcal{R} = \{r_{\theta,W} : z \in \mathbb{R}^d \mapsto \theta^T z + g_W(z), \\ \theta \in \mathbb{R}^d, \quad g_W \text{ feed-forward NN with weights } W\}$$

Recovering the identity $r_{\theta,W}(z) = \theta^T z + g_W(z)$ we can simply note that $g_W(z) = r_{\theta,W}(z) - \theta^T z$. This means that the deep learning contribution to the AFT model accounts for what linearity cannot explain. This is the idea behind the working principle of Residual Networks, which have been proven to be universal approximators (Lin and Jegelka, 2018).

We outline in Algorithm 1 a new optimization routine inspired by LassoNet’s HIER-PROX (Lemhadri et al., 2021). The whole optimisation problem is defined therein as

$$\begin{aligned} & \underset{\sigma, \theta, W}{\text{minimize}} && L(\sigma, \theta, W) := -l_n(\sigma, \theta, W) + \lambda \|\theta\|_1 \\ & \text{subject to} && \|W_j^1\|_\infty \leq M |\theta_j|, j = 1, \dots, d, \end{aligned}$$

where W_j^1 denotes the outward weights for feature j in the first hidden layer. The objective is minimised via the technique of hierarchical proximal optimisation.

The proposed architecture integrates both linear transformations and a perceptron-based model acting on the input data. This dual-component structure offers a flexible way to capture different sparse patterns in data thanks to the constrained optimization problem above. However, it is important to note that the architecture introduces non-identifiability: there is no control on the signal proportion absorbed by each part, making it challenging to disentangle the unique contributions of each. While this does not harm the predictive power of the model, it offers an avenue for future research on interpretability and model decomposition.

Because of the ℓ^1 -penalty placed on the objective function, the linear contribution of many input covariates is being shrunk to zero. The constraint imposes that the first hidden layer weights associated with such covariates are also being shrunk to zero. This fact has true regularization implications, as the non-linear effects of covariates that are screened by the linear Lasso scheme vanish all the way down forward propagation throughout the hidden layers. We provide an adaptation that makes compatible the optimization of the interval-censored likelihood with deep learning automatic differentiation computational libraries such as `torch.autograd` (Paszke et al., 2019)¹. The high level algorithm is given in Algorithm 1 below.

Algorithm 1 Optimization routine derived from (Lemhadri et al., 2021)

- 1: Initialize $\theta^{(0)}$, $W^{(0)}$, $\sigma^{(0)}$, number of epochs B , hierarchy multiplier M , learning rate α , number of iterations K
 - 2: **for** $k \in \{1 \dots K\}$ **do**
 - 3: Compute gradient of loss function w.r.t (σ, θ, W) using back-propagation
 - 4: Update $\sigma \leftarrow \sigma - \alpha \nabla_\sigma L$, $\theta \leftarrow \theta - \alpha \nabla_\theta L$ and $W \leftarrow W - \alpha \nabla_W L$
 - 5: Update $(\theta, W^1) \leftarrow \text{HIER-PROX}(\theta, W^1, \alpha\lambda, M)$
 - 6: **end for**
-

2.2.2 Stability selection

Stability selection (Meinshausen and Bühlmann, 2010) is a powerful method for estimating discrete structures and performing variable selection, especially in high-dimensional data contexts. The main challenge

¹ https://pytorch.org/tutorials/beginner/blitz/autograd_tutorial.html

in such scenarios is finding the right amount of regularization to achieve an optimal model size. To address this issue, stability selection uses a subsampling strategy to assess variable selection stability across different data subsets, enabling control over the expected number of falsely selected variables. This method improves the accuracy of variable selection and provides a new structure estimation scheme.

In our case, we are leveraging the non-deterministic variable selection process of neural networks, which in other grid-search-based methods would constitute a computationally infeasible task. The initialization of the network's weights introduces a beneficial level of randomness that can be more effectively utilized in our setting.

One critical advantage of stability selection is its ability to provide a guarantee on the expected number of false selections, under certain assumptions (Meinshausen and Bühlmann, 2010). Stability selection involves repeatedly subsampling a dataset without replacement, each time applying a variable selection method under varying levels of regularization. For each regularization level, it counts how frequently each variable is selected across these subsamples. By setting a threshold on this frequency, one can ensure that the expected number of falsely selected variables is bounded, thus enhancing the reliability of the variable selection process. This method provides a principled way to choose the regularization parameter, thereby controlling the rate of false discoveries in the model.

Assuming that the distribution of selected variables is exchangeable and the original procedure is no worse than random guessing, the expected number of falsely selected variables can be bounded:

$$E(V) \leq \frac{1}{2\pi_{thr} - 1} \frac{q_\Lambda^2}{d},$$

where q_Λ is the average number of selected variables across the regularisation parameter set Λ , π_{thr} is the cutoff parameter and d is the total number of covariates as denoted throughout the rest of the paper.

Stability selection is a helpful tool for variable selection in high-dimensional data analysis. Traditional methods, such as cross-validation, can be challenging to use for deep learning problems in high-dimensional settings because the risk curve, which shows the relationship between the model complexity and prediction error, can be too noisy and hard to minimize. In contrast, stability selection uses subsampling to control the selection of variables and provides a more stable and interpretable solution.

2.3 Predictive model

Regression models serve as essential tools for understanding relationships among variables. They allow for the assessment of interaction terms, non-linear effects, and other complex relationships within the data.

In this operating mode of our proposed method, the regression function will be approximated by elements $r_W \in \mathcal{P}$, being \mathcal{P} the space of feedforward neural networks with no skip layer

$$\mathcal{P} = \{r_W : z \in \mathbb{R}^d \mapsto g_W(z), g_W \text{ feed-forward NN with weights } W\}.$$

Unlike variable selection, which primarily focuses on reducing dimensionality and identifying significant predictors, predictive modeling extends our analytical capabilities.

2.4 Sample-splitting

Our multi-stage regression method involves three steps, following a similar lens to (Wasserman and Roeder, 2009). A generic way for performing high-dimensional regression consists on splitting the sample with indices $\{1, \dots, n\}$ into a partition D_1, D_2 and D_3 .

1. Stage I. Use D_1 to find $\hat{S}(D_1) \subset \{1, \dots, p\}$ using stability selection.
2. Stage II. Use the subsample D_2 and the selected variables $\hat{S}(D_1)$ to find the low dimensional estimate $r_{\hat{W}}$ for model $\hat{S}(D_1)$.

3. Stage III. Use D_3 and $r_{\hat{W}}$ to test the performance of the model on unseen data using C-index (Harrell et al., 1982).

An scheme for our proposal is the following:

$$\underbrace{\text{sample} \xrightarrow{\text{stage I}} \hat{S}(D_1)}_{\text{train}} \xrightarrow{\text{stage II}} r_{\hat{W}} \xrightarrow{\text{stage III}} \underbrace{\text{C-index}}_{\text{test}}.$$

We make explicit the third step involving evaluation on a fresh dataset, in contrast with classical splitting structures (Dezeure et al., 2015).

3 Simulated experiments

In this paper, we have opted for the most straightforward configuration to maintain clarity and facilitate illustration. We fix F to be the standard normal cdf and $\phi(t) = \log(t)$. This leads to the AFT $\log T = r_{\theta, W}(Z) + \varepsilon$, $r_{\theta, W} \in \mathcal{R}$ with $\varepsilon \sim \mathcal{N}(0, \sigma^2)$. The parameter space is

$$\Gamma = \{(\sigma, \theta, W) \in (0, +\infty) \times \mathbb{R}^d \times \mathbb{R}^N\}$$

where N is the total number of weights involved in the layers of the deep residual block.

While more complex settings could offer additional nuances, the aim here is to provide a transparent and easily interpretable analysis, thereby serving as a foundation for future studies that may wish to explore these complexities in greater depth.

3.1 Generation of interval-censored targets

We describe a method to simulate interval-censored data, resembling the scenarios encountered in medical studies with periodic checkups. A fixed number of checkup times (20) and the probability of attending the next checkup (0.5) are set.

The logarithm of latent event times is generated based on the mean vector (see further details below) plus random normal zero-mean noise. Each patient's checkup times are then randomly generated within a log-uniform distribution.

Next, an algorithm determines whether each checkup was attended before or after the latent event time. Based on this, it detects the nearest checkup time before and after the event. The delta indicators save whether the event time is left-censored, interval-censored or right-censored.

This synthetic data generation method closely mimics the data collection process in medical studies, where patients undergo periodic checkups, and the exact event time (like onset of a disease) is unknown but is bounded by these checkup times. This approach effectively creates interval-censored data, essential for testing and validating statistical models designed for such data structures.

3.2 Description of the simulation setups and results

We describe the structure of two simulated regression scenarios below. Example 1 generates the regression function according to the following model:

$$\log T = X_1 + X_1^2 - 0.5(X_2 + X_2^2) + 0.5(X_3 + X_3^2) + 1 + \varepsilon$$

where X_1, X_2, \dots, X_{100} are the predictor variables with $X_i \sim \mathcal{N}(0, 1)$ for $i = 1, 2, 3$. The error term is $\varepsilon \sim \mathcal{N}(0, \sigma^2)$, where $\sigma = 0.5$. The covariance matrix for the predictor variables is the identity.

For Example 2, let $\beta_0 = -2$, $\beta_1 = 0.5$, $\beta_2 = -0.7$, $\beta_3 = 0.8$, $\beta_4 = 0.6$, $\beta_5 = -0.3$, and $\sigma = 0.5$. We also specify the covariance matrix Σ for the predictor variables as $\Sigma_{i,j} = (-1)^{i-j} \rho^{|i-j|}$ where $\rho = 0.3$ and $i, j = 1, \dots, 100$. We then generate the predictor variables X_1, X_2, \dots, X_{100} by drawing a sample of

size n from a multivariate normal distribution with mean vector 0 and covariance matrix Σ . Finally, the true survival times T are calculated as a function of the predictor variables:

$$\begin{aligned} \log T = & \beta_0 + \beta_1 X_1 + \beta_2 X_2 + \beta_3 X_3 \\ & + \beta_4 X_1 X_3 + \beta_5 \log(X_2^2 + 1) \end{aligned} \quad +\varepsilon$$

where ε is a random error term drawn from a normal distribution with mean 0 and standard deviation σ .

To assess the variable selection performance of our proposed method in the two datasets described above, we generated 500 simulated replicas for each scenario, varying the sample size between $n = 500, 1000, 2000$. Stability selection was then run across 100 subsamples and 50 values of λ to estimate the stability paths of each simulation. Our results demonstrate that the variables were consistently and accurately selected, indicating the robustness and reliability of our method. See Figure 1 for a graphical illustration.

In the predictive regression experiments, we evaluate the performance of our method (Table 2) against `LogNormalAFTFitter` from the `lifelines`² (Davidson-Pilon, 2019) package (Table 3), using the same simulated datasets after manually removing irrelevant variables from the predictors. We measure the predictive accuracy in survival analysis using the concordance index (C-index, Harrell et al. (1982)), which is computed over a fresh test sample of the same size and generated by the same mechanism as the original dataset. C-index is computed as

$$C - index = \frac{\sum_{i \neq j} 1 \{ \eta_i < \eta_j \} 1 \{ t_i > t_j \} (1 - \delta_{3j})}{\sum_{i \neq j} 1 \{ t_i > t_j \} (1 - \delta_{3j})},$$

where η_k is minus the predicted conditional mean of log-survival time given by the fitted model; t_k is the mid-point of interval k in case of left or interval censoring and left border in case of right-censoring.

Additionally, we use the coefficient of determination R^2 , which measures the strength of the relationship between the predicted values of the AFT regression surface and the original noiseless logarithm of underlying times. To assess performance across simulated datasets, we average the metrics across simulation runs. Figure 1 demonstrates the effective discrimination of relevant and irrelevant variables in Example 1 using stability selection.

The key findings from the simulation section are summarized as follows:

- In Example 1, our method outperforms the `LogNormalAFTFitter` when clear nonlinearity in statistical association is present. Our model exhibits a 40% higher predictive power in terms of performance measures. Additionally, as the sample size increases, our model converges to the σ parameter, while the competitor deviates significantly from the true value due to model misspecification.
- In Example 2, when the data structure closely resembles linearity, both our proposal and the `LogNormalAFTFitter` yield comparable accuracy. Nonetheless, our model excels at capturing subtle nonlinearities, a capability beyond the reach of the competitor. Additionally, it successfully converges to the true value of the σ parameter.
- In both examples, the variable selection algorithms yield no false positives with $n = 2000$, and the true positives are correctly identified. This demonstrates that in these scenarios, the variables are detected accurately.

Overall, our proposal outperforms the competitor, even when the model is quasi-linear. This highlights the broader applicability of our approach in approximating more complex nonlinear regression functions and justifies the flexibility of our new framework.

² <https://lifelines.readthedocs.io/>

4 Practical considerations

The stability selection procedure requires a careful implementation to ensure its effectiveness when particularized to our proposal. This section outlines the framework that encapsulates the core algorithm, following the principles laid out in the original LassoNet (Lemhadri et al., 2021) and stability selection (Meinshausen and Bühlmann, 2010) papers, with adaptations to suit our specific context and to enhance interpretability of results. This implementation allows users to effectively explore the relationship between the proportion of selected variables (q_λ/p) and the selection frequency of each feature j (π_j^λ), while also providing a graphical framework for controlling the expected number of falsely selected variables.

Orientative limits for the lambda grid are set based on a preliminary whole path run (see Section 4.1 in Lemhadri et al. (2021)). For each subsampling draw, a distinct path is created. Next, we iterate through the selection states of all paths at each lambda value. During each iteration, the average selection probability for each variable is calculated across all models. Importantly, we ensure that the selection probability for each variable is monotonically decreasing as we progress through the lambda values. At each step, we take the element-wise minimum between the current selected and the new average selection probability. The outcome of this process is that the selection probability curves for each variable will be monotonically decreasing across the lambda values. Subsequently, we plot³ $(\pi_1^\lambda, \dots, \pi_p^\lambda)$ against $\frac{q_\lambda}{p}$.

We recall the bound for the expected number of falsely selected variables under the assumptions in Theorem 1:

$$E(V) \leq \frac{1}{2\pi_{thr} - 1} \frac{q_\Lambda^2}{p}$$

Dividing both sides by p , we obtain

$$\frac{E(V)}{p} \leq \frac{1}{2\pi_{thr} - 1} \frac{q_\Lambda^2}{p^2} =: F\left(\frac{q_\lambda}{p}\right)$$

Let us define $x := \frac{q_\lambda}{p}$. Then, for each bound F on the expected proportion of falsely selected variables $\frac{E(V)}{p}$, we derive a family of curves indexed by F :

$$\pi_{thr}(x) = \frac{1}{2} \left(\frac{x^2}{F} + 1 \right).$$

Finally, we can add these curves to the $(\pi_1^\lambda, \dots, \pi_p^\lambda)$ against $\frac{q_\lambda}{p}$ plot to identify which variables would be selected upon fixing the false discovery rate upper bound F we are willing to accept, see Figure 3.

5 Application of the Method in the Type 1 Diabetes Exchange Registry Dataset

Survival analysis modeling is a powerful statistical approach used in medical research to understand the occurrence time-to-event clinical events, such as death and the development of diseases as the case of Diabetes Mellitus. In the case of diabetes researchers, survival analysis plays an important role in the control, definition, and establishment of new therapeutic strategies for this heterogeneous metabolic syndrome. For example, the cutoff of the biomarker glycosylated hemoglobin [A1c] (a surrogate measure of

³ This approach follows the guidance provided in the original stability selection paper, which states: “To do this, we need knowledge about q_Λ . This can be easily achieved by regularization of the selection procedure $\hat{S} = \hat{S}^q$ in terms of the number of selected variables q , i.e., the domain Λ for the regularization parameter λ determines the number q of selected variables, i.e., $q = q(\Lambda)$. For example, with l_1 -norm penalization as in expressions (2) or (4), the number q is given by the variables which enter first in the regularization path when varying from a maximal value λ_{max} to some minimal value λ_{min} . Mathematically, λ_{min} is such that $|\cup_{\lambda_{max} \geq \lambda \geq \lambda_{min}} \hat{S}^\lambda| \leq q$.”

the glucose values of the preceding 3 months of glucose values) to diagnose diabetes Mellitus was derived from survival analysis models in terms from diabetes complications.

From a technical perspective, diabetes disease is diagnosed and monitored with lab measures that are only collected between consecutive medical visits. Then, the different clinical events that are defined in diabetes clinical practice and by diabetes researchers lead to outcomes represented as interval-censored variables. To illustrate the importance of analyzing interval-censoring outcomes and to continue our discussion on the significance of these models in diabetes research, we proceed with a real example in this domain.

In this study, our focus is on quantifying the progression of type 1 diabetes, particularly in terms of renal complications—a crucial criterion for considering the use of more intense and specific pharmacological treatments with therapeutic benefits, albeit accompanied by more secondary adverse effects.

Here, the use of survival models to analyze the statistical associations between various risk factors and time-to-event outcomes serves multiple purposes in translational clinical research: i) managing type 1 diabetes effectively; ii) improving the metabolic glucose capacity of the patients; iii) minimizing mortality rates associated with type 1 diabetes; iv) reducing healthcare costs. Specifically, we measure the time until reaching a low albuminuria concentration, a critical surrogate marker for renal function specified in each medical lab test of the patients. The outcome exhibits an interval-censored structure because the clinical event happens between two consecutive medical examinations.

For our analysis, we leverage data from the T1D Exchange, publicly available at <https://t1dexchange.org/>. The dataset includes information from 5971 patients, and the variables selected by our approach are summarized in Table 1.

Our primary goal is to create a risk score, represented as an Accelerated Failure Time (AFT) regression surface, for predicting the development of albuminuria concentration disorders in type 1 diabetes patients. Before showing AFT results, we start with a descriptive analysis that provide content to the sample analyzed.

A descriptive analysis in the groups of patients that experienced the clinical event and those who did not reveals that the range of age involves patients with juvenile diabetes type 1 and all age ranges include elderly patients. For each example in the corresponding groups for age and BMI, the 25-75% quantiles are 7.0 and 69.4, respectively, for individuals who experienced the event of interest. Conversely, for those who did not experience the event, these quantiles are 6.0 and 63.0. This trend aligns with the general expectation that older individuals are more prone to developing renal complications, suggesting age as a potential risk factor. Regarding BMI, the distribution appears relatively stable across both groups. Among those who experienced the event, the 2.5% and 97.5% quantiles for BMI are 15.5 and 38.0, respectively. In contrast, for individuals who remained at risk by the end of the study, these quantiles are 15.4 and 36.4. This similarity in the distribution of BMI across groups indicates that BMI might not undergo significant changes in relation to the observed event, suggesting a lesser or different role of BMI compared to age in the context of this study's event of interest.

To explore the temporal component when the clinical event occurred, Figures 5 and 6 present stratified Turnbull estimators categorized by A1c levels and treatment indicators, respectively. For A1c levels, we stratify the patients into well-controlled and poorly controlled diabetes patients. The marginal survival analysis indicates that fitting integrated regression models with several patient factors must be done to analyze the joint patient characteristics.

After fitting the new neural network approach and comparing it with a classical AFT model with a log-normal distribution, our new models outperform traditional linear log-normal AFT models, achieving a concordance index of 0.65 compared to the traditional approach's 0.54. The concordance index was computed using a 20 percent left-fresh sample to assess the accuracy of both models. A summary of the selected variables can be found in Table 1.

Our neural network learning-based approach offers preliminary valuable guidelines for delaying renal complications as indicated by disorders in albuminuria concentration. From a practical standpoint, our model identifies key variables such as A1c levels (a summary variable of the patients in the previous

three months) and insulin dosage (the standard clinical treatment in this setting), providing a nuanced understanding of their impact on time-to-disorder. Figure 6 suggests that to achieve better outcomes, it is crucial to maintain minimal levels of both A1c and insulin dose. Additionally, we observe that angiotensin-converting enzyme (ACE) inhibitors and angiotensin receptor blockers (ARBs) have a modifying effect on the benefits of insulin administration.

In cases of high A1c levels, insulin administration can delay time-to-pathology, and this beneficial effect is more significant in patients who take angiotensin-converting enzyme (ACE) inhibitors or angiotensin receptor blockers (ARBs). Patients with diabetes may require insulin therapy to help control their blood glucose levels. ACE inhibitors and ARBs are medications used to treat hypertension and heart failure, which block the action of angiotensin to reduce blood pressure and also have additional benefits such as reducing inflammation and improving insulin sensitivity. In general, in the realm of type 1 diabetes management, achieving optimal patient outcomes is a multifaceted challenge involving various pharmacological interventions and lifestyle modifications (Lewis et al., 2001), and our model provides new clinical knowledge about potential therapeutic interactions regarding A1c and insulin levels.

In summary, our analysis reveals the following key findings: i) the predictive advantages of our model compared to Accelerated Failure Time (AFT) linear models in this application; ii) the sparsity of the underlying model, emphasizing the paramount importance of variable selection; iii) in the context of diabetes applications, the necessity to consider non-linear models due to the non-linear interactions illustrated in Figure 6; iv) the use of a larger pool of biomarkers and information from continuous glucose monitoring may be required to improve predictive capacity (Matabuena et al., 2021).

Table 1 Variable characteristics in the T1DX data.

Variable	T1DX code	Description	Support	Selected
1	ageConsent	Age at consent date (years)	Continuous	no
2	Pt_Gender	Gender	0: male, 1: female	no
3	BldPrSys	Systolic blood pressure	Continuous	no
4	BldPrDia	Diastolic blood pressure	Continuous	no
5	ACEARB	Taking ACE inhibitors or AR blockers	0: no, 1: yes	yes
6	WeightKg	Participant weight in kilograms	Continuous	no
7	HeightCm	Height at exam (cm)	Continuous	no
8	diabDur	Duration of T1D (years)	Continuous	no
9	TotalDailyInsPerKg	Total daily insulin dose per kg	Continuous	yes
10	LDL	LDL value	Continuous	no
11	HDL	HDL value	Continuous	no
12	TotChol	Total cholesterol value	Continuous	no
13	Triglyc	Triglycerides value	Continuous	no
14	HbA1c	HbA1c	Continuous	yes
15	isletCellTrans	Participant had an islet cell transplant	0: no, 1: yes	yes
16	bmi	BMI	Continuous	no
17	NumPumpBolusOrShortActUnk	Unknown number of boluses or insulin injections	1: checked	yes

6 Discussion

This paper introduces a novel methodological contribution by presenting a new deep AFT model class for interval-censored targets. We introduce a novel variable selection strategy that leverages sparse neural networks, which is integrated in the regression algorithm. To the best of our knowledge, this is one of first methods combining the interval-censoring paradigm with deep learning algorithms. Given the prevalence of interval-censoring in personalized medicine applications, this model holds great relevance in this domain. The diverse results presented in this paper substantiate its value as an extension of classical AFT modelling while retaining interpretability advantages.

Our work paves the way for new and exciting research directions in the field of interval-censoring. This includes addressing the noise distribution of AFT non-parametrically (Pang et al., 2021). Moreover, there

is a growing need to provide measures of uncertainty for new predictions, particularly in medical science applications, where patient evolution inherently involves uncertainty. We propose extending conformal inference ideas to the interval-censoring setup, building upon existing approaches for right-censored data and split conformal inference methods (Izbicki *et al.*, 2022). Another intriguing possibility is to accommodate functional predictors such as medical images or wearable signals—a largely unexplored area with significant implications for digital medicine applications (Matabuena and Petersen, 2023; Ghosal *et al.*, 2023). For example, in our diabetes applications, the use of continuous glucose monitoring can improve the capacity prediction to detect long-term diabetes complications.

Furthermore, establishing the significance of each selected variable represents another crucial research direction. Recently, post-selection methodologies for neural networks have emerged, and they can be applied to our model (Zhu *et al.*, 2021).

Appendix: NHANES physical activity data

The National Health and Nutrition Examination Survey (NHANES) is a comprehensive program conducted by the National Center for Health Statistics (NCHS), with the primary objective of collecting health and nutrition data from the United States population. In this study, we utilized a subset of $n = 2977$ patients aged between 50 and 80 years, gathered from NHANES waves 2003-2006. This subset contains valuable data on physical activity patterns, measured with Actigraph accelerometry technology during 3-7 days with a time-resolution of one record per minute.

From a public health and epidemiological perspective, establishing a statistical association between physical activity and mortality in the elderly population is of paramount importance. This analysis can serve as the foundation for promoting healthy habits across the population and designing targeted interventions to mitigate the adverse effects of inactivity and the natural decline in functional capacity that occurs with aging (Leitzmann *et al.*, 2007; Zhao *et al.*, 2020). Furthermore, given that physical inactivity is a modifiable risk factor for various chronic diseases, including heart disease, diabetes, and specific types of cancer, the implementation of effective physical activity policies has the potential to extend the lifespan of this at-risk population, enhance their quality of life, and significantly reduce healthcare costs while alleviating the burden on the medical infrastructure.

The objectives of our analysis are twofold. First, from the list of variables in Table 4- containing multiple physical activity summaries derived from accelerometers- and other patient characteristics, we aim to identify a reduced subset of variables that maximizes predictive capacity. Second, we assess the variable selection capabilities of our approach and evaluate the efficacy of our predictive algorithm by comparing it with the traditional Accelerated Failure Time (AFT) log-normal model, assessing the capacity of our prediction model in creating time-to-event risk scores.

To evaluate these objectives, we randomly divide the sample into a training set (80% of the total) and a test set (the remaining 20%) and run both our approach and the benchmark model using the variables listed in Table 4. In our proposal, we further split the 80% training set into two 40% sets. The first part of the training sample is used for stability selection, and a low-dimensional fit is performed using the selected predictors in the second part of the sample. The performance of both models is evaluated using the concordance index on the remaining 20% of the sample. Table 4 displays the variables selected by our model, and the estimated stability paths are shown in Figure 7.

Our results are highly relevant in the domain of physical activity. Among the variables introduced in Table 4, which include basic patient characteristics and a range of physical activity summaries, only the moderate to vigorous activity variable and some summaries of physical activity during the central time of the day are relevant in identifying patients with lower survival. These results align with the existing scientific literature, emphasizing the importance of moderate-to-vigorous physical activity (Stamatakis *et al.*, 2022) and the significance of monitoring physical activity to identify increased risks across various diseases due to inactivity and transitions between inactivity and activity during the day (Schrack *et al.*, 2019).

Figure 8 illustrates the survival curves predicted by our model for variables such as gender, age, mobility problem, and active-to-sedentary transition probability when fixing the rest of the covariates to zero. Notably, non-constant spacing of these conditional curves between consecutive values of the covariates reveals non-linearity in their dependence with survival.

In conclusion, our approach yields a higher concordance index of 0.79 compared to the traditional linear log-normal AFT model, which produces a concordance index of 0.75. These findings demonstrate the superior performance of our approach in predicting survival outcomes while comprehensively selecting the most relevant variables. Moreover, the use of variable selection algorithms allows us to identify the most relevant physical activity summaries in predicting patient survival, a topic of significant interest. As a next step, we suggest extending our algorithm to introduce modern distributional representations of accelerometer data as functional covariates, thereby addressing some limitations associated with using summaries (Matabuena and Petersen, 2023).

References

- Bagdonavicius, V. and Nikulin, M. (2001). *Accelerated life models: modeling and statistical analysis*. CRC press.
- Cho, H., Jewell, N. P., and Kosorok, M. R. (2021). Interval censored recursive forests. *Journal of Computational and Graphical Statistics*, 31(2):390–402.
- Davidson-Pilon, C. (2019). lifelines: survival analysis in python. *Journal of Open Source Software*, 4(40):1317.
- Dezeure, R., Bühlmann, P., Meier, L., and Meinshausen, N. (2015). High-dimensional inference: confidence intervals, p -values and R-software hdi. *Statistical Science*, 30(4):533 – 558.
- Efron, B. (1967). The two sample problem with censored data. In *Proceedings of the fifth Berkeley symposium on mathematical statistics and probability*, volume 4, pages 831–853.
- Gentleman, R. and Geyer, C. J. (1994). Maximum likelihood for interval censored data: Consistency and computation. *Biometrika*, 81(3):618–623.
- Ghosal, R., Matabuena, M., and Zhang, J. (2023). Functional proportional hazards mixture cure model with applications in cancer mortality in NHANES and post ICU recovery. *Stat Methods Med Res.*, 32(11):2254–2269.
- Harrell, Frank E., J., Califf, R. M., Pryor, D. B., Lee, K. L., and Rosati, R. A. (1982). Evaluating the Yield of Medical Tests. *JAMA*, 247(18):2543–2546.
- Hothorn, T., Bühlmann, P., Dudoit, S., Molinaro, A., and Van Der Laan, M. J. (2005). Survival ensembles. *Biostatistics*, 7(3):355–373.
- Huang, J. (1996). Efficient estimation for the proportional hazards model with interval censoring. *The Annals of Statistics*, 24(2):540 – 568.
- Huang, J. and Wellner, J. A. (1997). Interval censored survival data: A review of recent progress. *Proceedings of the First Seattle Symposium in Biostatistics: Survival Analysis, Lecture Notes in Statistics*, 123.
- Izbicki, R., Shimizu, G., and Stern, R. B. (2022). Cd-split and hpd-split: Efficient conformal regions in high dimensions. *Journal of Machine Learning Research*, 23(87):1–32.
- Jia, Y. and Jeong, J.-H. (2022). Deep learning for quantile regression under right censoring: Deepquantreg. *Computational Statistics and Data Analysis*, 165:107323.
- Lee, C., Zame, W., Yoon, J., and Van Der Schaar, M. (2018). Deephit: A deep learning approach to survival analysis with competing risks. In *Proceedings of the AAAI conference on artificial intelligence*, volume 32.
- Leitzmann, M. F., Park, Y., Blair, A., Ballard-Barbash, R., Mouw, T., Hollenbeck, A. R., and Schatzkin, A. (2007). Physical Activity Recommendations and Decreased Risk of Mortality. *Archives of Internal Medicine*, 167(22):2453–2460.
- Lemhadri, I., Ruan, F., and Tibshirani, R. (2021). LassoNet: A neural network with feature sparsity. *Journal of Machine Learning Research*, 22(127):1–29.
- Lewis, E. J., Hunsicker, L. G., Clarke, W. R., Berl, T., Pohl, M. A., Lewis, J. B., Ritz, E., Atkins, R. C., Rohde, R., and Raz, I. (2001). Renoprotective effect of the angiotensin-receptor antagonist irbesartan in patients with nephropathy due to type 2 diabetes. *New England Journal of Medicine*, 345(12):851–860. PMID: 11565517.
- Lin, H. and Jegelka, S. (2018). Resnet with one-neuron hidden layers is a universal approximator. *Advances in Neural Information Processing Systems*, 31.

- Maathuis, M. H. and Wellner, J. A. (2008). Inconsistency of the MLE for the joint distribution of interval-censored survival times and continuous marks. *Scand. Stat. Theory Appl.*, 35(1):83–103.
- Matabuena, M. and Petersen, A. (2023). Distributional data analysis of accelerometer data from the NHANES database using nonparametric survey regression models. *Journal of the Royal Statistical Society Series C: Applied Statistics*, 72(2):294–313.
- Matabuena, M., Petersen, A., Vidal, J.C., and Gude, F. (2021). Glucodensities: A new representation of glucose profiles using distributional data analysis. *Stat Methods Med Res.*, 30(6):1445–1464.
- Meinshausen, N. and Bühlmann, P. (2010). Stability selection. *Journal of the Royal Statistical Society: Series B (Statistical Methodology)*, 72(4):417–473.
- Pang, M., Platt, R. W., Schuster, T., and Abrahamowicz, M. (2021). Spline-based accelerated failure time model. *Statistics in Medicine*, 40(2):481–497.
- Paszke, A., Gross, S., Massa, F., Lerer, A., Bradbury, J., Chanan, G., Killeen, T., Lin, Z., Gimelshein, N., Antiga, L., Desmaison, A., Kopf, A., Yang, E., DeVito, Z., Raison, M., Tejani, A., Chilamkurthy, S., Steiner, B., Fang, L., Bai, J., and Chintala, S. (2019). Pytorch: An imperative style, high-performance deep learning library. In Wallach, H., Larochelle, H., Beygelzimer, A., d'Alché-Buc, F., Fox, E., and Garnett, R., editors, *Advances in Neural Information Processing Systems*, volume 32. Curran Associates, Inc.
- Rindt, D., Hu, R., Steinsaltz, D., and Sejdinovic, D. (2022). Survival regression with proper scoring rules and monotonic neural networks. In *International Conference on Artificial Intelligence and Statistics*, pages 1190–1205. PMLR.
- Schrack, J. A., Kuo, P.-L., Wanigatunga, A. A., Di, J., Simonsick, E. M., Spira, A. P., Ferrucci, L., and Zipunnikov, V. (2019). Active-to-sedentary behavior transitions, fatigability, and physical functioning in older adults. *The Journals of Gerontology: Series A*, 74(4):560–567.
- Sen, B. and Xu, G. (2015). Model based bootstrap methods for interval censored data. *Computational Statistics and Data Analysis*, 81:121–129.
- Stamatakis, E., Ahmadi, M. N., Gill, J. M., Thøgersen-Ntoumani, C., Gibala, M. J., Doherty, A., and Hamer, M. (2022). Association of wearable device-measured vigorous intermittent lifestyle physical activity with mortality. *Nature Medicine*, 28(12):2521–2529.
- Steingrimsson, J. A. and Morrison, S. (2020). Deep learning for survival outcomes. *Statistics in medicine*, 39(17):2339–2349.
- Sun, J. (2006). *The statistical analysis of interval-censored failure time data*, volume 3. Springer.
- Sun, T. and Ding, Y. (2023). Neural network on interval-censored data with application to the prediction of Alzheimer's disease. *Biometrics*, 79(3):2677–2690.
- Tibshirani, R. (1996). Regression shrinkage and selection via the lasso. *Journal of the Royal Statistical Society: Series B (Methodological)*, 58(1):267–288.
- Travis-Lumer, Y. and Goldberg, Y. (2021). Kernel machines for current status data. *Machine Learning*, 110(2):349–391.
- Turnbull, B. W. (1976). The empirical distribution function with arbitrarily grouped, censored and truncated data. *Journal of the Royal Statistical Society: Series B (Methodological)*, 38(3):290–295.
- Van de Geer, S. (1993). Hellinger-consistency of certain nonparametric maximum likelihood estimators. *The Annals of Statistics*, 21(1):14–44.
- Wasserman, L. and Roeder, K. (2009). High-dimensional variable selection. *The Annals of Statistics*, 37(5A):2178 – 2201.
- Wei, L.-J. (1992). The accelerated failure time model: a useful alternative to the Cox regression model in survival analysis. *Statistics in medicine*, 11(14-15):1871–1879.
- Wu, Y. and Cook, R. J. (2020). Assessing the accuracy of predictive models with interval-censored data. *Biostatistics*, 23(1):18–33.
- Yao, W., Frydman, H., and Simonoff, J. S. (2019). An ensemble method for interval-censored time-to-event data. *Biostatistics*, 22(1):198–213.
- Yu, Q., Li, L., and Wong, G. Y. (2000). On consistency of the self-consistent estimator of survival functions with interval-censored data. *Scandinavian Journal of Statistics*, 27(1):35–44.
- Zhang, Y., Hua, L., and Huang, J. (2010). A spline-based semiparametric maximum likelihood estimation method for the Cox model with interval-censored data. *Scandinavian Journal of Statistics*, 37(2):338–354.

- Zhao, M., Veeranki, S. P., Magnussen, C. G., and Xi, B. (2020). Recommended physical activity and all cause and cause specific mortality in us adults: prospective cohort study. *BMJ*, 370.
- Zhong, Q., Mueller, J., and Wang, J.-L. (2022). Deep learning for the partially linear Cox model. *The Annals of Statistics*, 50(3):1348 – 1375.
- Zhong, Q., Mueller, J. W., and Wang, J.-L. (2021). Deep extended hazard models for survival analysis. *Advances in Neural Information Processing Systems*, 34.
- Zhu, Z., Fan, Y., Kong, Y., Lv, J., and Sun, F. (2021). Deeplink: Deep learning inference using knockoffs with applications to genomics. *Proceedings of the National Academy of Sciences*, 118(36):e2104683118.

Table 2 Performance of our proposal averaged across $B = 500$ simulations

Example 1			
n	c-index	R^2	$\hat{\sigma}$
500	0.8118	0.9647	0.3812
1000	0.8165	0.9776	0.4527
2000	0.8198	0.9857	0.4732
Example 2			
n	c-index	R^2	$\hat{\sigma}$
500	0.8110	0.9499	0.4139
1000	0.8156	0.9670	0.4596
2000	0.8192	0.9773	0.4868

Table 3 Performance of the competitor averaged across $B = 500$ simulations

Example 1			
n	c-index	R^2	$\hat{\sigma}$
500	0.6784	0.5664	1.8120
1000	0.6808	0.5659	1.8405
2000	0.6854	0.5702	1.8428
Example 2			
n	c-index	R^2	$\hat{\sigma}$
500	0.8142	0.9173	0.8960
1000	0.8144	0.9180	0.9129
2000	0.8152	0.9179	0.9320

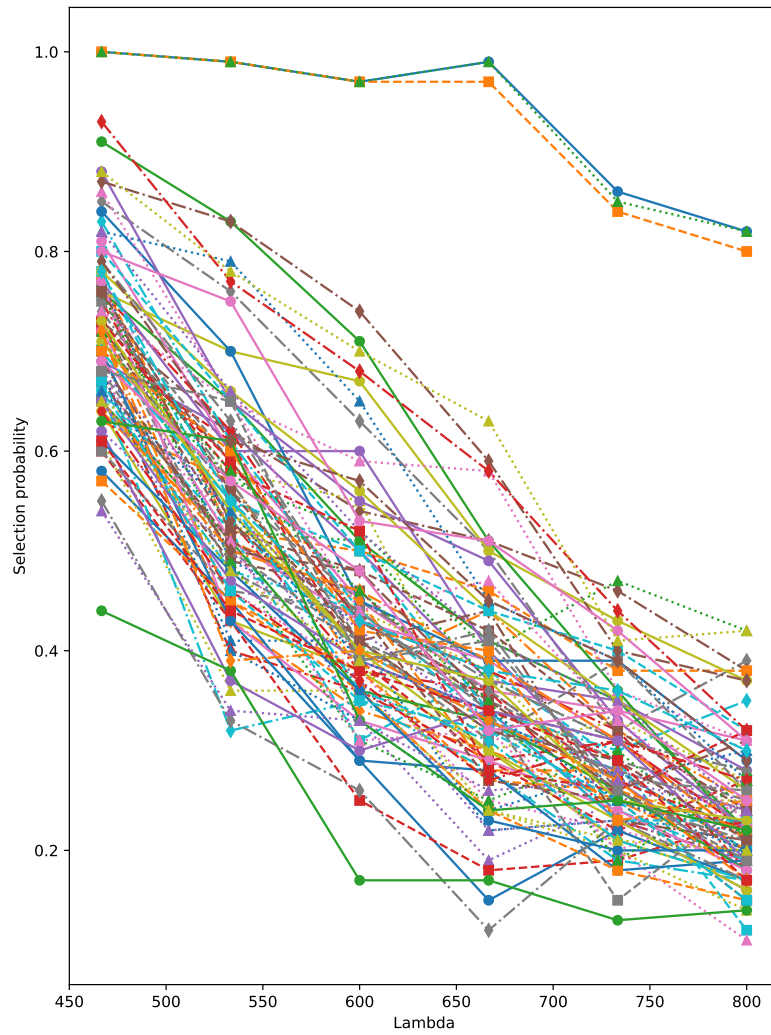


Figure 1 The stability selection technique applied to synthetic data: example 1 with $n = 1000$.

Figure 2 Example diagram of a feedforward neural network with a skip layer. The architecture used in the application to NHANES data would be the same, adding an extra layer with the same number of hidden units (10). The total number of parameters, in that case, is 604. Bias terms are omitted in the drawing.

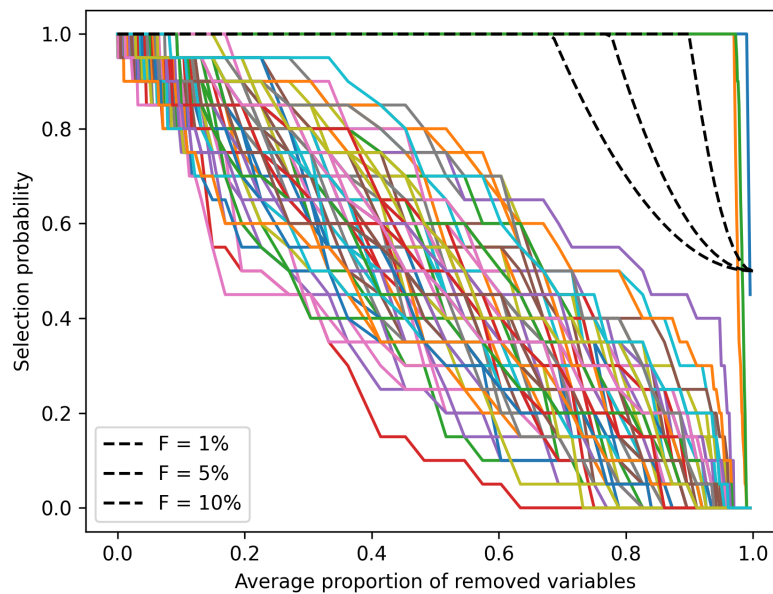
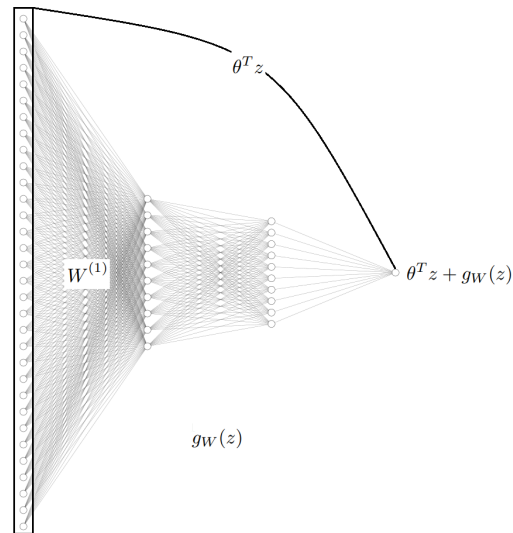


Figure 3 Graphical deliverable of Section 4. For a desirable expected proportion of removed variables x and a false discovery rate F both fixed by the user, the variables eventually entering the model are the ones whose frequency curve π_j surpasses the dotted black line given by F at x

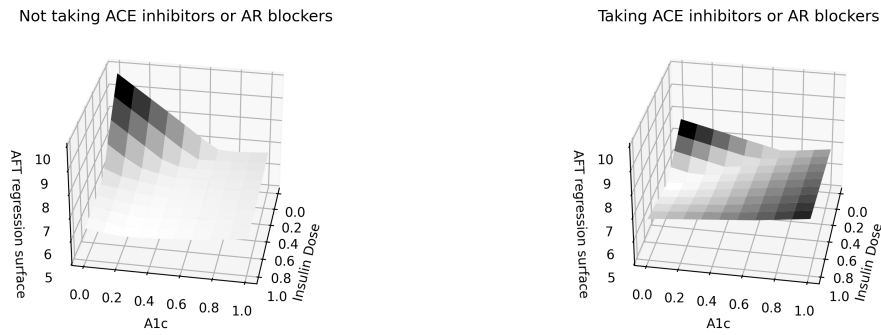


Figure 4 Predicted regression surface of our neural AFT model upon setting all the covariates to baseline value except from A1c and received units of insulin. Each plot corresponds to setting the treatment indicator to 0 or 1 in addition respectively, being the arms labeled in the title of the plots. Minimum and maximum values of these covariates are encoded in the plot as 0 and 1 respectively. This figure pictures the general idea that, if certain assumptions are met, neural networks can capture complex, non-linear interactions between features without explicitly modeling them. Logarithm of survival time as a function of these two variables is already highly non-linear per se, and when a third categorical variable comes into play we see that the regression surface is not modified by a simple shift. For the control arm, it is harder to reduce risk of albuminuria concentration disorder by providing insulin to patients with high values of A1c.

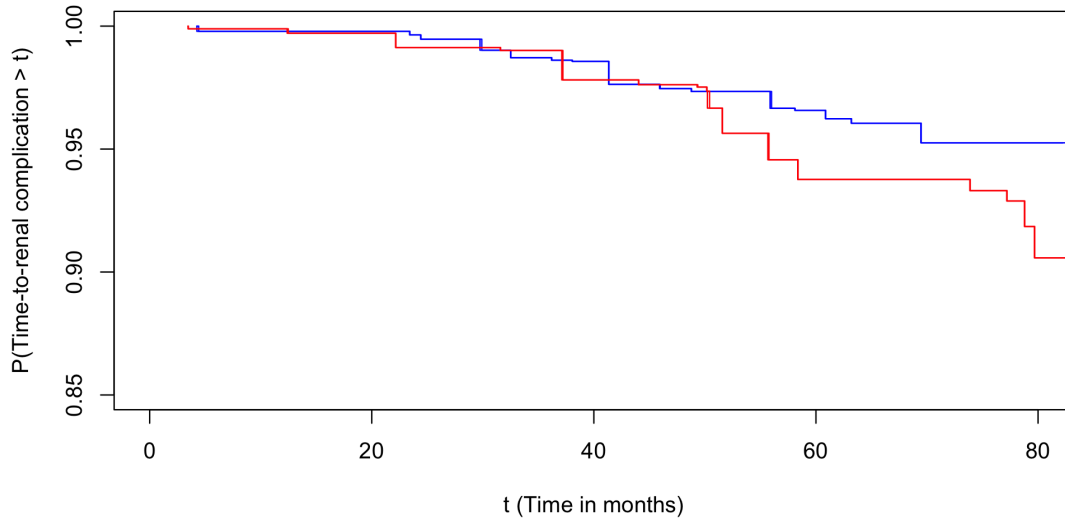


Figure 5 Marginal Turnbull estimators stratified by HbA1c values. Blue curve encompasses data satisfying $\text{HbA1c} < 8$ and red involves observations such that $\text{HbA1c} \geq 8$.

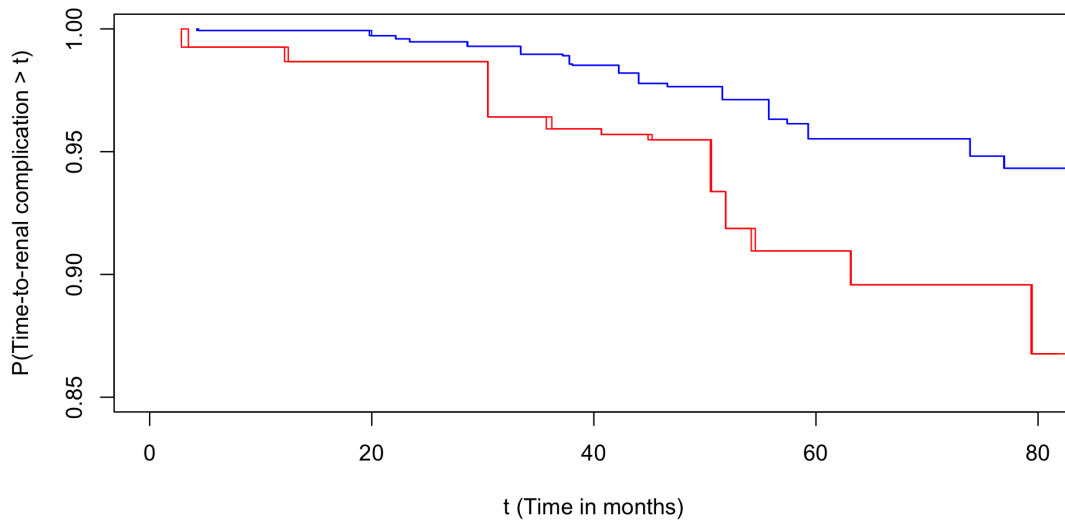


Figure 6 Marginal Turnbull estimators stratified by treatment indicator. Blue curve encompasses patients who did not take ACE inhibitors or AR blockers and red involves individuals who did.

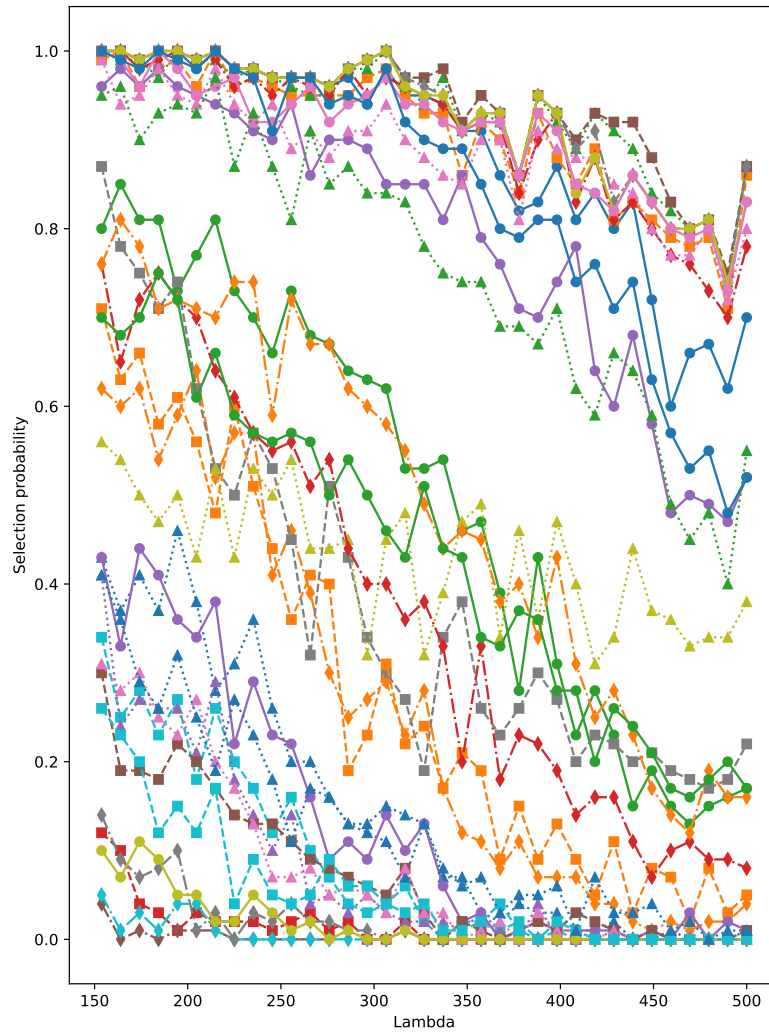


Figure 7 The stability selection paths for NHANES data. Each color represents a different covariate in Table 4. The expected number V of falsely selected variables is bounded by $E(V) \leq \frac{1}{2\pi_{thr}-1} \frac{q_{\Lambda}^2}{p}$. Setting q_{Λ} - the expected number of selected variables to 10 and π_{thr} to 0.95 we have $E(V) \leq 4$.

Table 4 Variable characteristics in the NHANES data.

Variable	NHANES code	Description	Support	Selected
1	Gender		0: Male, 1: Female	yes
2	Cancer		0: no, 1: yes	yes
3	Stroke		0: no, 1: yes	yes
4	Diabetes		0: no, 1: yes	yes
5	BMI		0: Normal, 1: Overweight	yes
6	CHF	Congesive Heart Failure	0: no, 1: yes	yes
7	CHD	Coronary Heart Disease	0: no, 1: yes	yes
8	Mobility Problem		0: no, 1: yes	yes
9	RIDAGEYR	Age at the interview time	Continuous	yes
10	LBXTC	Total Cholesterol	Continuous	no
11	LBDHDD	Direct HDL-Cholesterol	Continuous	no
12	SYS	Systolic Blood Pressure	Continuous	no
13	TAC	Total volume of physical activity	Continuous	no
14	TLAC	Total log activity counts	Continuous	no
15	WT	Accelerometer wear time	Continuous	no
16	ST	sedentary Time	Continuous	no
17	MVPA	Moderate-to-Vigorous Physical Activity	Continuous	yes
18	ABout		Continuous	no
19	SBout		Continuous	no
20	SATP	Sedentary-to-active transition prob.	Continuous	no
21	ASTP	Active-to-sedentary transition prob.	Continuous	yes
22	TLAC ₁	Total log activity counts 12AM-2AM	Continuous	no
23	TLAC ₂	Total log activity counts 2AM-4PM	Continuous	yes
24	TLAC ₃	Total log activity counts 4PM-6PM	Continuous	no
25	TLAC ₄	Total log activity counts 6PM-8PM	Continuous	no
26	TLAC ₅	Total log activity counts 8PM-10PM	Continuous	no
27	TLAC ₆	Total log activity counts 10PM-12PM	Continuous	no
28	TLAC ₇	Total log activity counts 12PM-2AM	Continuous	no
29	TLAC ₈	Total log activity counts 2AM-4AM	Continuous	no
30	TLAC ₉	Total log activity counts 4AM-6AM	Continuous	no
31	TLAC ₁₀	Total log activity counts 6AM-8AM	Continuous	no
32	TLAC ₁₁	Total log activity counts 8AM-10AM	Continuous	no
33	TLAC ₁₂	Total log activity counts 10AM-12AM	Continuous	no

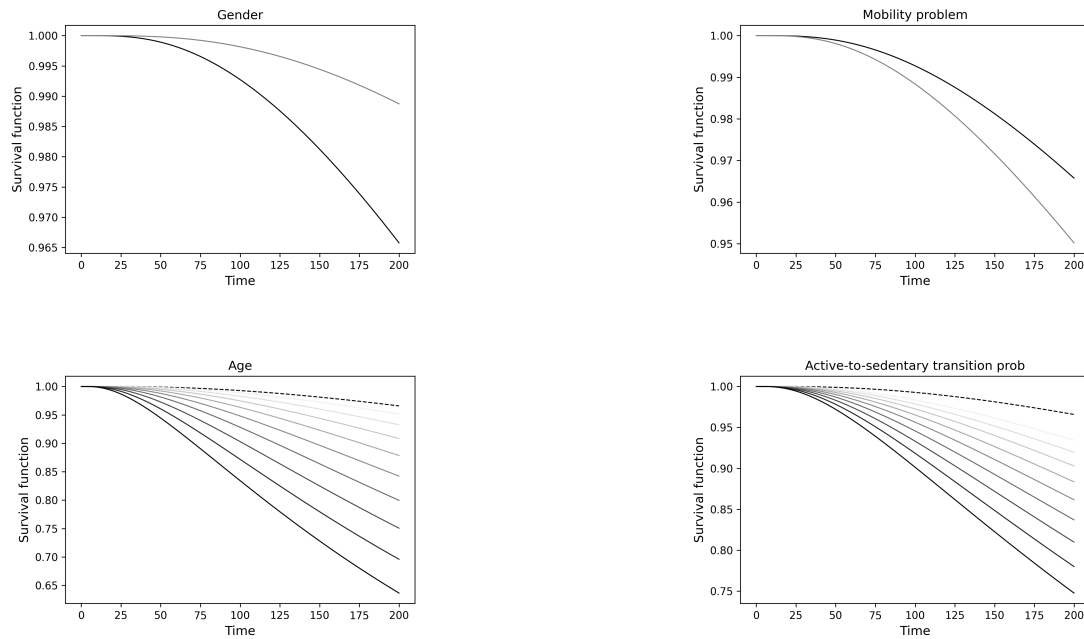


Figure 8 Estimated survival functions for several configurations of the covariates (time scale in months). Note that the dashed graph, the baseline survival function, is the same across all the plots. In (c), the different curves were estimated by doing forward passes of different ages through our model keeping the rest of the variables at zero. More intense greys correspond to higher ages, and the darkest solid grey corresponds to the age of the oldest person in the dataset. The same idea holds for (d), but varying ASTP and setting the rest of the covariates to zero. In (a), grey stands for female and black for male. In (b), grey stands for suffering from a mobility problem and black stands for the opposite. First hints of non-linearity can be perceived in that the grid of different age values on which predictions of the corresponding survival curves were launched was equally-spaced, whereas the estimated curves are not.